

On the stall flutter occurrence in a blade cascade set to turbine and compressor geometry

Pavel Procházka^{1*}, Pavel Šnábl¹, Sony Chindada¹, Ondřej Bublík² and Václav Uruba^{1,3}

¹The Czech Academy of Sciences, Institute of Thermomechanics, Dolejškova 5, Praha 8, CR

²UWB, FAS, Department of Mechanics, Universitní 8, Plzeň, CR

³UWB, FME, Department of Power System Engineering, Universitní 8, Plzeň, CR

Abstract. A blade cascade allowing free pitch movement of five blades was developed in Institute of Thermomechanics. This model is introduced to study the phenomenon of stall flutter existing in rotary bladed wheels of steam turbines and other devices. This article describes how to induce the stall flutter for prescribed boundary conditions (as inlet velocity, various angles of attack, etc.) and gives survey about flow field differences around the cascade set to both the turbine and the compressor geometry. This experimental research utilized time-resolved Particle Image Velocimetry (PIV) to measure and to evaluate statistical quantities of the wake behind the NACA0010 profiles of the cascade. Also dynamical analysis was performed in the form of Fast-Fourier transform and also phase-locked measurement was applied. Gained knowledge will be utilized to design advanced model of the cascade allowing stall flutter examination without the use of ball bearings.

1 Introduction

A low structural and aeroelastic damping plays crucial role in the case of last stage blades (LPT) because the blades are very long and the profile of this tip region has very sharp edges and low curvature. More, these blades have no shroud to minimize the centrifugal forces. The (stall) flutter phenomenon can occur in the case of such rotary periodical bodies arising from aeroelastic coupling between the structural vibrations and aerodynamic instabilities. Especially stall flutter is very dangerous phenomenon since it would lead to high-cycle fatigue and consequently to fast failure of the whole device. This fact must be taken into account during the design of rotary bladed wheel as well as during the operation.

This article describes a partial goal of the project dealing with nonlinear stall flutter of flexible profiles with pitch degree of freedom in subsonic flow to get more information about fluid-structure interaction (FSI) as flutter is very important part of aeroelasticity examined in turbomachinery [1]. The effect of aeroelastic coupling is commonly studied using three different approaches. The profiles can be subjected to flow instabilities and are self-oscillating [2] or profiles are exposed to kinematic excitation [3] or force excitation. This project combines the first and the last approach. This research follows on previous presented one [4, 5, 6] where the plunge degree of freedom of blades was utilized. However, the plunge motion is not able to cause such strong aeroelastic coupling because

the flow separation does not occur when the blade vertical position is changing.

To prevent the stall flutter of the cascade, complex CFD models should be developed which could help during the design process. It is essential to model the velocity (pressure) field for proper modelling of aeroelastic coupling. However, CFD model could fail for some conditions as various angles of attacks (AoAs) and hence it should be validated using results from measurement in physical models. The model of such five-blade cascade is visible in figure 1 and its description will be present in the next chapter. There are some discrepancies between PIV data and two different CFD models (see figure 3a, b, c, d). The subjected quantity is velocity profiles plotted 100 mm behind the cascade (in the wake). As the comparison looks very promising (Fig. 2) for positive AoAs or zero value (compressor arrangement), for negative incidence angles situation differs. It seems that the process is more viscous in reality than in simulations. Obviously, the flow field is very complex in the vicinity of the cascade, there is a strong dependency on incoming angles and the dynamic activity is very important and it should be studied primarily by PIV method.

2 Experimental setup and CFD models

A two-dimensional model of rotational periodic body, which is a blade cascade, was built and placed inside a plexiglass channel connected to the blow-down wind tunnel facilities. This physical model was used to

* Corresponding author: prochap@it.cas.cz

perform time-resolved PIV measurement as well as force measurement. Five blades with profile NACA 0010 were used in the cascade geometry - profile chord length was 72.8 mm, stagger angle equal to 30° and vertical blade distance 16.14 mm. The first and last blade was auxiliary. Three middle blades were allowed to have pitch motion. The blade was supported by a shaft only at one end. The shaft has led through one side wall of the test section and necessary equipment (springs, bearings, encoders) were located aside the channel. A circular rotating table was used to allow AoA setting from -15° to $+15^\circ$. More, each blade could be compensated regarding static force affecting the AoA value within the cascade. The shakers were used to prescribe periodic harmonic motion of the pitch degree of freedom. The blade vibration was controlled with feedback loop to oscillate with the precise amplitude so we could get close to kinematic excitation. The forces (aerodynamic, inertia and elastic) were measured using the force transducer B&K type 8203. The blade position was acquired by miniature magnetic rotary encoder RLS RM08. These data were saved by Yokogawa ScopeCorder DL750. The transparent test section was connected to the tunnel orifice with cross-sectional dimension 100 x 250 mm. Although many regimes with different velocity were tested, this article will deal with the velocity equal to 20 m/s.

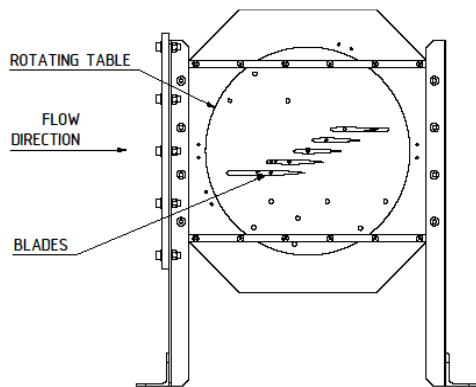


Fig. 1. Assembly of the blade cascade with a rotary disc.

The flow field was measured by PIV apparatus from Dantec company. To illuminate the tracing particles (oil droplets), laser New Wave Pegasus Nd:YLF with double-head was used (frequency 10 kHz, wavelength 527nm, energy in one pulse 10mJ for 1 kHz). Fast PIV camera Phantom V611 (up to 6000 double snaps per second, spatial resolution 1280x800 pix, memory 8 GB) was used to capture the particle movement. The system synchronization is performed via timer box. Dynamic Studio ver. 3.4 was utilized to capture the data and post-process data. Adaptive correlation with embedded validation was used to calculate velocity vector maps. An interrogation area of 16x16 pixels resulted in 159x99 vectors (maximal 5% invalid vectors). Further data analysis and plotting was performed in Matlab or in Tecplot software.

The acquisition frequency differs for individual purpose. The frequency for mean flow quantities evaluation and for higher statistical moments was set to

100 Hz during 10 seconds of recording. To detect and to analyse rapid flow fluctuation especially in the wake, the sampling frequency was set to 2 kHz. The motion of excited blade demonstrates periodic motion and the flow in the close vicinity has also pseudo-periodic character. To suppress the random component and to highlight the periodic component of the flow is very convenient to use a phase-locked measurement. The sampling frequency is set as a product of excitation frequency and the number of desired phases per one period. The dataset of each phase is then averaged over all periods resulting in mean phase velocity and its standard deviation (STD).

The regime with fixed blades is referred as base case. It is introduced here especially for comparison with CFD. One regime was studied with freely supported blades, but no free oscillation was observed. The periodic motion was prescribed by pitch amplitude equal to 3° , frequency of motion was 40 Hz and different inter-blade phase angle (0° or 180°) was set.

Numerical simulations were calculated using Ansys Fluent and FlowPro open-source CFD software. Ansys utilized compressible $k-\omega$ SST turbulence model. The fluid parameters were set to corresponding real values in the wind tunnel (viscosity ratio 1, inlet turbulence intensity 0.1% etc.). FlowPro is a multipurpose CFD software developed for complex fluid simulations as vibrating blades in a steam turbine. It utilized the incompressible fluid model together with Spalart-Allmaras turbulence model. The fluid parameters were set same as for Fluent solver.

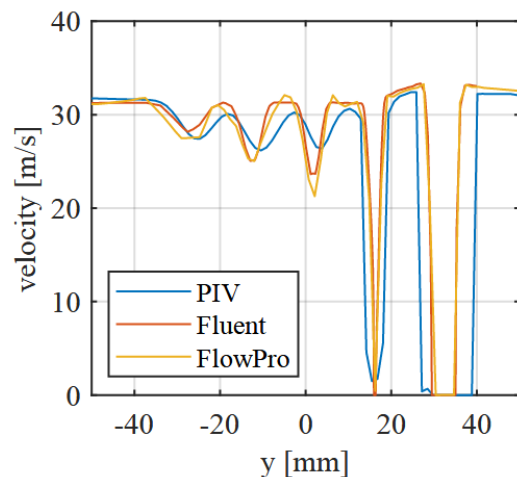


Fig. 2. Velocity profile comparison 100 mm behind for 0° .

3 Results

The coordinate system is set so that the origin is in the leading edge of the middle blade (3rd) in its hypothetical position with zero angle of attack. The vector field is depicted using black vector representing both velocity components in the plane of measurement. The color is used to plot the scalar value (mainly vector modulus). The flow is coming from the left side. A compressor arrangement of the cascade is represent by positive angle of attack 10° . Contrary, the turbine setup is characterized by negative value -12° .

3.1 CFD x PIV

There is a comparison for PIV data and data from Ansys and FlowPro for zero AoA in figure 2. The distribution of mean velocity across the channel behind the cascade can be simulated quite credibly. The position of wakes as well as the peak values corresponds for all three approaches. The situation is much more complicated when the AoA is negative (Fig. 3a). The velocity profiles do not corresponds at all. Nor the peak values either the wake position. It seems that the flow in CFD calculation is less viscous. The numerical model has big problem to detect the huge separation at the very first profile and also the wake itself (see figure 3b, c, d). It is obvious that the flow dynamics in the case of moveable profile will become much more complicated to predict. Further in the article, we will describe the flow topology and dynamics inside the cascade using PIV. There is a mean flow field distribution for compressor and turbine setup in the figure 4a,b. Compressor arrangement shows the detail of the 3rd, 4th and 5th blade. On the other hand, turbine arrangement shows the inter-blade channels between 1st, 2nd and 3rd profile. The FFT analysis is performed to detect frequencies present in the flow. The analyzed point coordinates are [80;-3] mm and [50;-3] mm for positive and for negative AoA, respectively. Both positions correspond to place of expected high activity of aeroelastic coupling. The point is chosen so it is between two moveable blades and in the vicinity of the trailing edge of preceding profile. It is obvious that the velocity value distribution differs completely for both cases. There is big separation of boundary layer at suction side of the first profile of the turbine blade cascade. The suction side is not fully covered by pressure side of adjacent blade in turbine setup and hence the flow separation is present more often. Also the mean velocity magnitude in inter-blade channel is higher than velocities present in compressor setup. However, this features is strongly influenced by the fact that blockage factor is much higher for negative values of AoA. Blades arranged in compressor cascade are located rather in a row behind each other and they are not distributed across channel height.

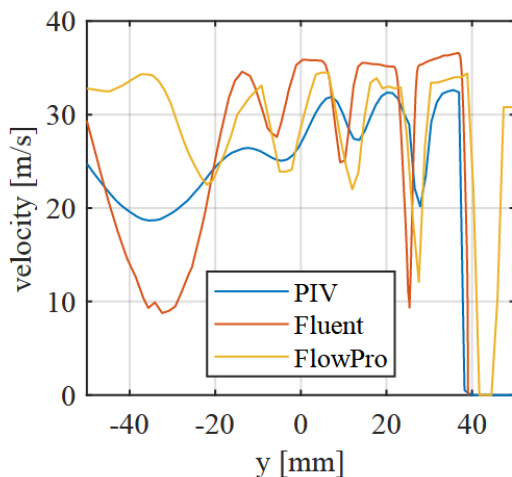


Fig. 3a. Velocity profile comparison 100 mm behind for -8° .

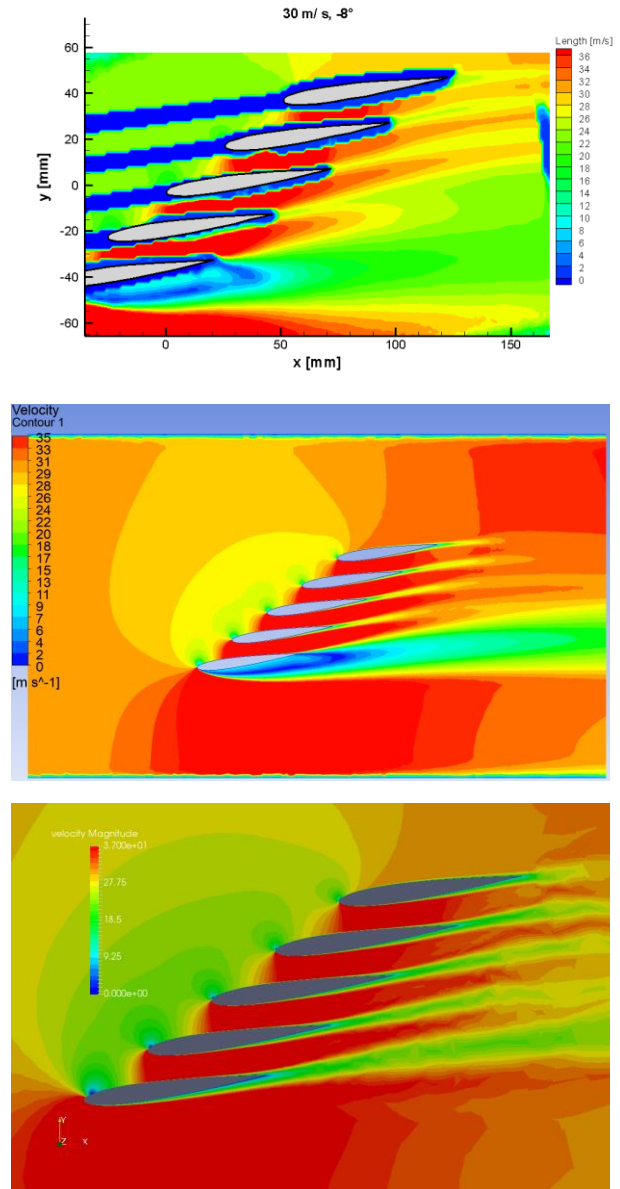
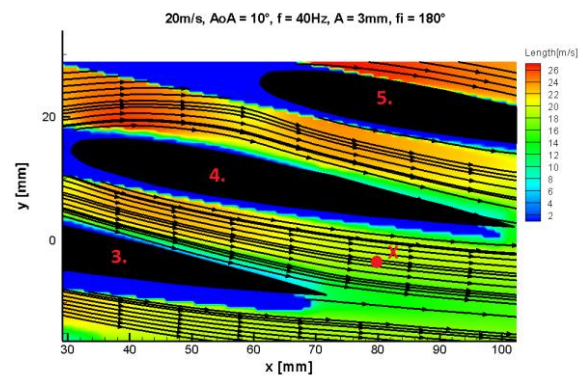


Fig. 3b, c, d. PIV, Fluent and FlowPro comparison, AoA -8° , velocity 30 m/s, distribution of mean flow velocities.



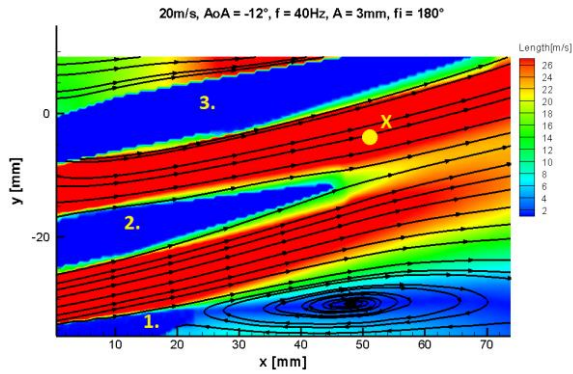


Fig. 4a, b. PIV measurement of compressor and turbine cascade, velocity distribution, vector lines, X-point location.

3.2 Flow dynamics

There are velocity variations in time, and frequency spectra for horizontal and vertical velocity component evaluated at point X for case with no excitation and negative AoA in figure 5. The blades are not fluttering, only insignificant vibrations were measured using sensitive encoders. There is no dominant frequency peak up to 50 Hz (plotted) and even no peak in higher frequencies. Further in article, we will search for PSD (power spectral density) value higher than one.

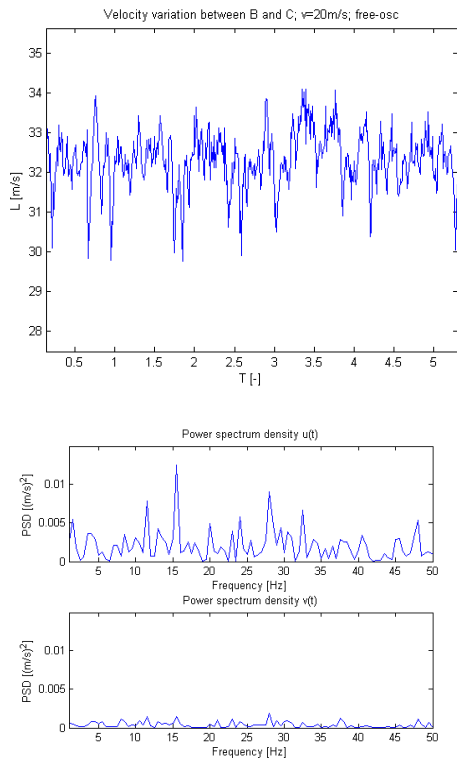


Fig. 5. Velocity variation and freq. spectra for both vel. components at point X for free-oscillating blades (turbine).

Further FFT analyses were performed for both type of cascades and for two values of inter-blade phase angle $\phi = 0^\circ$ and 180° at point X. The dominant frequency 40 Hz was detected for all cases. It is evident that this

frequency is embedded to the flow field by the excitation frequency. Both values are exact the same! There is an example (Fig. 6, 7) of instantaneous velocity in time and frequency spectra for both cascades and ϕ equal to 180° . The mean velocity value is about 19 m/s and 32 m/s for positive and negative AoA, respectively. The peak PSD value is about 1.5 for both cases and dominates for horizontal velocity component.

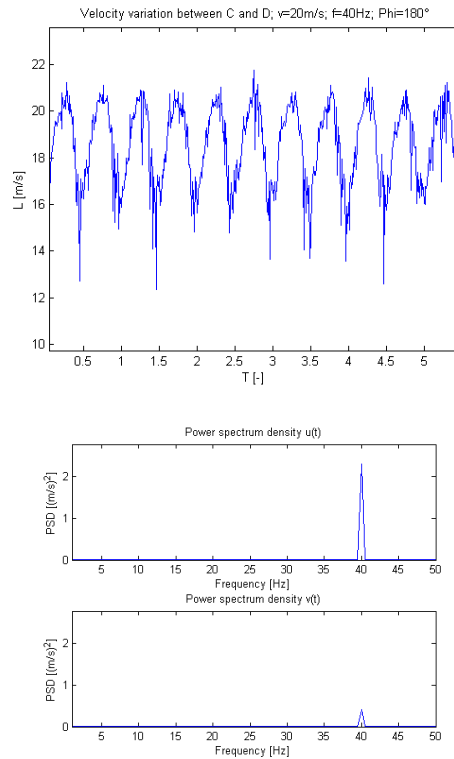


Fig. 6. Velocity variation and freq. spectra for both vel. components at point X for excited blades (compressor).

Next step is to plot the PSD value distribution in the whole plane of measurement for the most dominant frequency 40 Hz to search for the highest aeroelastic activity region. Only the result gained for phase angle 180° will be presented to maintain the article clarity. For this phase angle, the adjacent moveable blades are performing its movement in antiphase motion and hence the interaction between them is higher compared to case when blades go simultaneously. The PSD value distribution for horizontal and vertical component can be seen in figure 8 for positive AoA of cascade. The red area (PSD value higher than 5) can be detected as region with very strong aeroelastic activity. The horizontal velocity component dominates over vertical one for all regimes. The highest activity is present between 3rd and 4th blade below its leading edge. This is caused by the fact that the channel width variations are quite significant here – the blades rotate against each other. Not so high activity is also present in the wake behind the middle blade. Unfortunately, the arbitrary chosen point X is located in the region with rather small activity (blue bubble below 4th blade). The coupling is even stronger for case of turbine setup (Fig. 9). The area between the leading edge of the middle blade and

adjacent blade has the same reason to exist as in former case. More, there is strong activity between the body of middle blade and both wakes from 1st and 2nd blade. The wake itself behind the 1st blade is huge (Fig. 4) and velocity variations are happening with exact frequency of 40 Hz despite the fact that this blade is fixed. Again the point X is outside the region with highest activity.

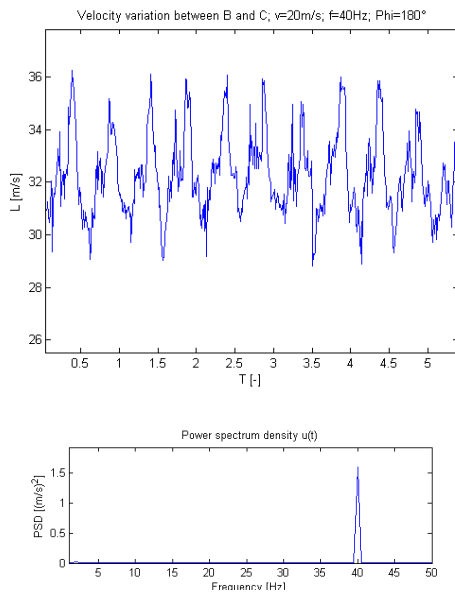


Fig. 7. Velocity variation and freq. spectra for one vel. component at point X for excited blades (turbine).

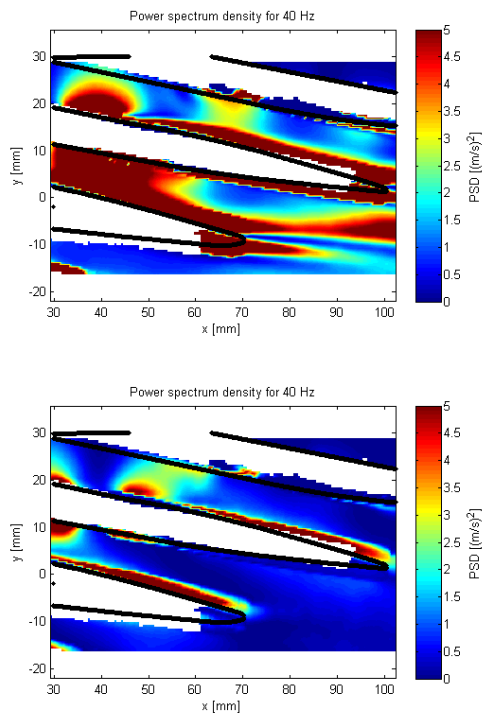


Fig. 8a, b. PSD value distribution for 40 Hz for both vel. components for compressor cascade, excited at $\phi = 180^\circ$.

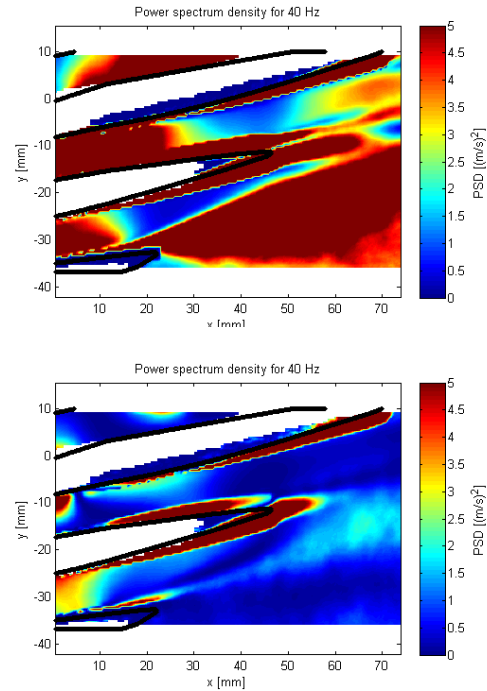


Fig. 9a, b. PSD value distribution for 40 Hz for both vel. components for turbine cascade, excited at $\phi = 180^\circ$.

3.3 Phase-locked measurement

The phase-locked measurements were conducted in distinct eight phases per period of harmonic motion prescribed by the shakers. The amplitude of this motion was set to 3° , so phase positions of the middle blade were set out in this order: $10^\circ-11.5^\circ-13^\circ-11.5^\circ-10^\circ-8.5^\circ-7^\circ-8.5^\circ$ for compressor setup. Notice, that the distribution is regular, e.g. the first and the fifth phase has the same position of the middle blade (and also adjacent blades). The phase positions were: $12^\circ-10.5^\circ-9^\circ-10.5^\circ-12^\circ-13.5^\circ-15^\circ-13.5^\circ$ with negative sign for turbine setup. The mean phase velocity in the plane of measurement was evaluated for all eight phases as well as standard deviation (STD) of this quantity.

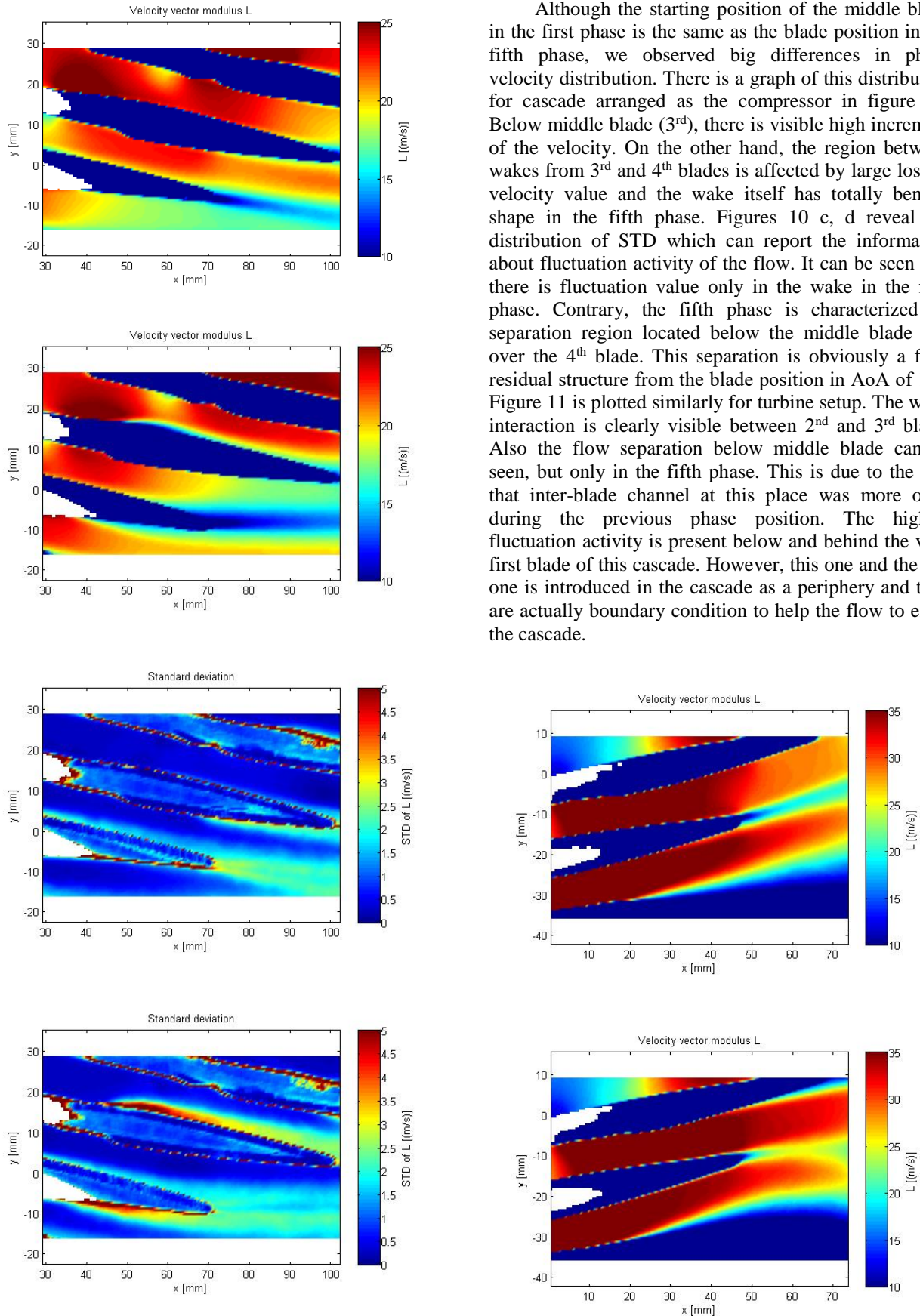


Fig. 10a, b, c, d. Mean phase velocity distribution and its STD value for excited regime (40 Hz and $\varphi = 180^\circ$) for compressor cascade.

Although the starting position of the middle blade in the first phase is the same as the blade position in the fifth phase, we observed big differences in phase velocity distribution. There is a graph of this distribution for cascade arranged as the compressor in figure 10. Below middle blade (3rd), there is visible high increment of the velocity. On the other hand, the region between wakes from 3rd and 4th blades is affected by large loss of velocity value and the wake itself has totally bended shape in the fifth phase. Figures 10 c, d reveal the distribution of STD which can report the information about fluctuation activity of the flow. It can be seen that there is fluctuation value only in the wake in the first phase. Contrary, the fifth phase is characterized by separation region located below the middle blade and over the 4th blade. This separation is obviously a flow residual structure from the blade position in AoA of 13° . Figure 11 is plotted similarly for turbine setup. The wake interaction is clearly visible between 2nd and 3rd blade. Also the flow separation below middle blade can be seen, but only in the fifth phase. This is due to the fact that inter-blade channel at this place was more open during the previous phase position. The highest fluctuation activity is present below and behind the very first blade of this cascade. However, this one and the last one is introduced in the cascade as a periphery and they are actually boundary condition to help the flow to enter the cascade.

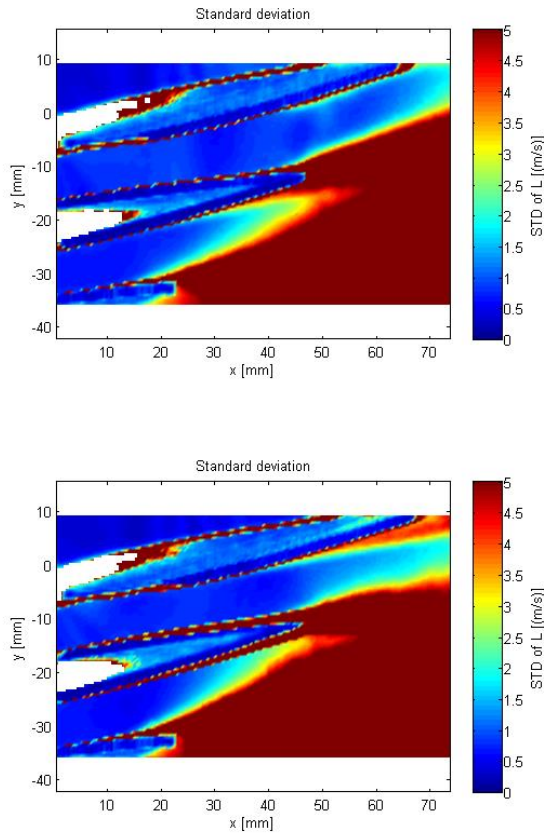


Fig. 11a, b, c, d. Mean phase velocity distribution and its STD value for excited regime (40 Hz and $\varphi = 180^\circ$) for turbine cascade.

4 Conclusions

The stereoscopic TR-PIV measurement was conducted inside the model composed of five NACA 0010 profiles (blades) in the shape of a cascade with stagger angle equal to 30° . This assembly allowed to change the angle of attack from -15° to $+15^\circ$. The important differences in flow field topology were observed for two standard cases; negative AoA simulating turbine arrangement and also positive AoA simulating a compressor. The comparison of statistical flow quantities with two CFD models was performed. Identified discrepancies will be resolved in the future.

During further investigation, the three middle blades were excited using three shakers, rotational harmonic motion with prescribed frequency 40 Hz and amplitude equal to 3° was introduced with different values of inter-blade phase angle. Dynamical analysis was utilized to search for regime and areas with important aeroelastic coupling. The phase angle equal to 180° is characterized by the existence of considerable FSI between blades motion and the flow properties as the channel between two adjacent blades is periodically expanding and narrowing which results in boundary layer separation.

Results evaluated from phase-locked measurements have shown that it is also very important

if the channel between two blades is opening or closing. The flow topology is actually affected by previous state of cascade geometry quite significantly. Generally it can be said, that the highest interaction between two blades are within areas, where the inter-blade channel can get the narrowest which is close to the leading edge or more downstream in the wakes.

The obtained results will be used to design advanced model of the blade cascade allowing to investigation of stall flutter by means of self-induced vibrations.

This work was supported by the research project of the Czech Science Foundation No. 20-26779S “Study of dynamic stall flutter instabilities and their consequences in turbomachinery application by mathematical, numerical and experimental methods” An institutional support RVO61388998 is also gratefully acknowledged.

References

1. J. J. Waite, Physical Insight, Steady Aerodynamic Effects, and a Design Tool for Low-Pressure Turbine Flutter, AAT 10107521, **77-09(E)**, Duke University, 2016
2. V. Tsybalyuk, J. Linhart, XVII IMEKO World Congress, TC3 (2003)
3. J. Lepičovský, E. R. McFarland, V. R. Capece, T. A. Jett, R. G. Senyitko, NASA/TM-211894 (2002)
4. J. Vimmr, O. Bublík, A. Pecka, L. Pešek, The 13th ISAIF in Okinawa, ISAIF13-S-0089 (2017)
5. L. Půst, L. Pešek, International Journal of Bifurcation and Chaos, IJBC-D-16-00353R2 (2017)
6. P. Procházka, V. Uruba, L. Pešek, V. Bula, EPJ Web of Conf., **180** (2018) 02086